

# Real-Time Stochastic Kinodynamic Motion Planning via Multiobjective Search on GPUs

Brian Ichter<sup>1</sup>, Edward Schmerling<sup>2</sup>,  
Ali-akbar Agha-mohammadi<sup>3</sup>, and Marco Pavone<sup>1</sup>

<sup>1</sup> Stanford University, Department of Aeronautics and Astronautics  
Stanford, CA, 94305

<sup>2</sup> Stanford University, Institute for Computational and Mathematical Engineering  
Stanford, CA, 94305

<sup>3</sup> Qualcomm Research, San Diego, CA, 92121

{ichter, schmerling, pavone}@stanford.edu, aliagha@qti.qualcomm.com

**Abstract.** In this paper we present the PUMP (Parallel Uncertainty-aware Multi-objective Planning) algorithm for addressing the stochastic kinodynamic motion planning problem, whereby we seek a low-cost, dynamically-feasible motion plan subject to a constraint on collision probability (CP). As a departure from previous methods for chance-constrained motion planning, PUMP directly considers both CP and the optimization objective at equal priority when planning through the free configuration space, achieving an unprecedented combination of cost performance, certified safety, and speed. Planning is conducted through a massively parallel multiobjective search, here implemented with a particular application focus on GPU hardware. PUMP explores the configuration space while maintaining a Pareto optimal front of motion plans, considering cost and approximate collision probability. We introduce a novel particle-based CP approximation scheme, designed for efficient GPU implementation, which accounts for dependencies over the history of a trajectory execution. Upon termination of the exploration phase, PUMP performs a search over the Pareto optimal set of solution motion plans to identify the lowest cost motion plan that is certified to satisfy the CP constraint (according to an asymptotically exact estimator). We present numerical experiments for quadrotor planning wherein PUMP identifies solutions in ~100 ms, evaluating over one hundred thousand partial plans through the course of its exploration phase. The results show that this multiobjective search achieves a lower motion plan cost, for the same collision probability constraint, compared to a safety buffer-based search heuristic and repeated RRT trials.

**Keywords:** Planning under uncertainty, Multiobjective optimization, GPU motion planning

## 1 Introduction

Motion planning is a fundamental problem in robotics involving the computation of a path from an initial state to a goal state that avoids obstacles and optimizes an objective function [1]. While this problem has traditionally been considered in the context of deterministic systems without kinematic or dynamic constraints, revolutions in modern sensing, vision, and learning technology have allowed agile autonomous systems

to operate “off the factory floor” where these simplistic assumptions may no longer hold. This new planning paradigm requires systems to act quickly on new information in a manner that is both dynamically feasible and robust to uncertainties in sensing and actuation. Moreover, we seek robotic control policies that, in the pursuit of safe operation, do not cede too many of the performance gains available from recent advances in the field of asymptotically optimal motion planning. Proper consideration of trajectory cost (e.g., time, control effort, or some combination thereof) should bring policy optimization against the limits of safety design constraints; a well designed policy should therefore be situated on a Pareto optimal front representing the tradeoff between the competing objectives of performance and safety. In this work we address the stochastic kinodynamic motion planning problem (henceforth referred to as the SKP problem), previously studied in [2], whereby one seeks a low-cost reference trajectory to be tracked subject to a constraint on obstacle collision probability (CP). Towards this goal, we introduce the Parallel Uncertainty-aware Multiobjective Planning algorithm, a novel approach to planning under uncertainty that employs a multiobjective search to build a Pareto front of plans into the configuration space, actively considering both cost and an approximation of CP during exploration. This search identifies several high-quality trajectories to be considered for certification of CP-constraint satisfaction via Monte Carlo (MC) methods [2]. The final certification step is essential to guarantee the hard safety constraint in an SKP problem formulation; we do not allow satisfaction modulo a CP approximation or through an a priori strong collision avoidance term in the cost function. The key to enabling real-time solutions (i.e., with sub-second computation time) in this work lies in algorithm parallelization which leverages the computational power of modern GPU hardware and the development of a novel fast and accurate CP approximation strategy over motion plans.

*Related Work:* A variety of strategies have been studied for adapting robot operations to the presence of uncertainties, most of which incorporate feedback from sensors online in order to inform the robot’s actions. One choice is to formalize the planning problem as a partially observable Markov Decision Process (POMDP) [3, 4, 5]. This allows a planner to consider closed-loop control policies that map belief distributions over the robot state to appropriate actions. Considering POMDP problems in their full generality, however, has been recognized as extremely computationally intensive; [6] provides a method for remedying the complexity of state belief evolution over the application of a control policy. In that work the authors use local feedback controllers to regularize the belief state at certain waypoints in space in order to break the dependence on history. While effective for constructing control policies that can handle large uncertainties, this approach is limited in the context of trajectory optimization due to the required stabilization phases. For systems where robustness against large deviations is not a routine need (e.g., indoor quadrotor flight), a common alternative approach is to optimize over open-loop trajectories, producing control sequences which serve as control policies when augmented with a tracking controller. These reference trajectories are recomputed in a receding horizon fashion to address substantial tracking errors and environmental uncertainties. This is the control strategy advanced in [2, 7, 8, 9]; we note that high-frequency replanning [9] has been shown to yield greatly increased robustness for systems with significant uncertainty. These works view the problem through the lens of chance-constrained optimization [10], of which the SKP is one formulation, where trajectories are gauged by a metric of their safety in addition to cost. Computationally

efficient methods for the exact estimation of tracking policy CP were introduced in [2] for guiding trajectory optimization, however, the MCMP procedure in that work addresses the relationship between cost and CP only indirectly, employing a deterministic asymptotically optimal planner with a safety-buffer heuristic as a proxy for CP. An alternative approach is using parallel rapidly-exploring random trees (RRTs) to generate a large set of candidate trajectories for CP evaluation [7, 8, 9]; high trajectory quality is ensured only through exhaustivity. Briefly, MCMP is chiefly cost focused while parallel RRTs are chiefly safety focused; in this work we draw inspiration from the multiobjective planning literature to select reference trajectories for the SKP problem without compromising on cost when guaranteeing a hard safety constraint.

Previously, [11] identified a need to treat multiple objectives independently when optimizing path plans in settings subject to stealth and time constraints. Unfortunately, even with a known state space (e.g., given a graph of all possible states and motions), multiobjective search with just 2 objectives is NP-hard [12]. Thus a major tenet of this work is to leverage algorithm parallelization to exploit the computational breadth of GPU hardware. An early result in sampling-based motion planning showed that probabilistic roadmap methods are embarrassingly parallel [13], which later inspired implementation on GPUs [14]. Most recent works in parallelization of sampling-based motion planning have focused on specific bottleneck subroutines (such as collision checking and nearest neighbor search) [15, 16] or used AND-/OR-parallelism to adapt serial algorithms [9, 17, 18]. With non-sampling-based planning methods, GPUs have been used with potential field methods [19] and optimization-based approaches [20], however these methodologies are often not feasible when the obstacles in the configuration space cannot be explicitly represented [1] and may become computationally inefficient when considering uncertainty.

*Statement of Contributions:* In this work we present a new algorithm, named the Parallel Uncertainty-aware Multiobjective Planning algorithm (PUMP), capable of returning high quality solutions to the stochastic kinodynamic motion planning problem. At PUMP’s core is a multiobjective search that considers trajectory cost and an approximation of the collision probability together while exploring the configuration space to identify high-quality motion plans for later certification of constraint satisfaction. The additional computational burden of maintaining a Pareto front of plans is offset by leveraging massively parallel computing, enabled, in particular, by GPU hardware. As such the algorithm is developed to exploit the high-throughput architecture of GPUs which allows thousands of threads to execute concurrently.

The design of PUMP can be separated into three phases, each of which is well posed for application to GPUs. The first is a graph-building phase which constructs a representation of available motions within the free configuration space; this phase is inspired by probabilistic roadmap methods which have been shown to be embarrassingly parallel [13]. The second explores this graph through a multiobjective search, building a Pareto front of motion plans outward from the initial state by expanding in parallel the set of all frontier plans below a constantly increasing cost threshold. This expansion is followed by a dominance check that considers the cost and CP (approximated using a heuristic) of all plans arriving at the same state to aggressively remove those that are less promising. We note that propagating CP along a motion plan requires consideration of the uncertainty distribution conditioned on collision avoidance; for each partial motion plan we collapse the full shape of the uncertainty distribution to a single ap-

proximate CP value for dominance comparison in multiobjective search. We show that this heuristic works well in practice and is necessary for limiting search branching factor. Upon completion of this graph exploration phase, a bisection search is performed over the Pareto optimal set of plans reaching the goal according to their approximate CP. The intent of this third phase is to correct for any CP inaccuracy by computing an unbiased estimate of the collision probability using Monte Carlo-based methods [2] (an embarrassingly parallel process), in order to exactly certify that the final returned solution satisfies the problem constraint.

Through numerical simulations of a double integrator in a 3D workspace (representing the guidance dynamics of a quadrotor) equipped with a Linear-Quadratic Gaussian (LQG) reference tracking controller, we find that PUMP improves over Monte Carlo Motion Planning [2] and repeated RRT trajectory generation in terms of motion plan cost, given the same CP constraint, while returning results in a tempo compatible with real-time operation on the order of 100 ms. To achieve this run time, a new trajectory CP approximation method is presented, termed Half-Space Monte Carlo (HSMC). The method approximates collision probability of a given trajectory by sampling many realizations of a reference-tracking controller. Each of these realized trajectories is checked against a series of relevant half-spaces representing a simplified collision model allowing a fast, accurate, and trivially parallelized CP approximation strategy.

*Organization:* This paper is structured as follows. Section 2 contains a formal definition of the stochastic kinodynamic motion planning problem addressed in this work. Section 3 outlines previous collision probability approximation methods and presents the novel HSMC method. Section 4 discusses the PUMP algorithm and Section 5 describes its implementation and presents simulation results supporting our statements. Lastly, Section 6 draws some conclusions and suggests directions for future work.

## 2 Problem Statement

This paper addresses the stochastic kinodynamic motion planning (SKP) problem posed in [2] which we briefly review here. We consider a robot described by linear dynamics with Gaussian process and measurement noise which tracks a nominal trajectory using a Linear-Quadratic Gaussian (LQG)-derived controller. Although PUMP with Monte Carlo simulation is equipped, as an algorithm framework, to handle problem formulations generalized to a nonlinear setup (as in, e.g., [8, 9] which base their computations on a local linearization around the reference trajectory) and to any tracking controller (e.g., LQG with nonlinear extended Kalman filter estimation, or geometric tracking control [21]), we focus our attention in this paper on demonstrating improvement in performance and speed over existing LQG methods. We note, however, that the Monte Carlo methods discussed in this work — in particular, all of their intermediate inputs computed from dynamics — are in principle directly applicable to a local linearization, or even non-Gaussian noise sampled, e.g., from zero-mean stable distributions.

The underlying nominal trajectory (and corresponding feedforward control term) is planned assuming continuous dynamics, but we assume discretized (zero-order hold) approximate dynamics for the tracking controller. That is, the robot’s dynamics evolve according to the stochastic linear model:

$$\dot{\mathbf{x}}(t) = A_c \mathbf{x}(t) + B_c \mathbf{u}(t) + \mathbf{v}(t), \quad \mathbf{y}(t) = C_c \mathbf{x}(t) + \mathbf{w}(t), \quad (1)$$

where  $\mathbf{x}(t) \in \mathbb{R}^d$  is the state,  $\mathbf{u}(t) \in \mathbb{R}^\ell$  is the control input,  $\mathbf{y}(t) \in \mathbb{R}^{d_w}$  is the workspace output, and  $\mathbf{v} \sim \mathcal{N}(\mathbf{0}, V_c)$  and  $\mathbf{w} \sim \mathcal{N}(\mathbf{0}, W_c)$  represent Gaussian process and measurement noise, respectively. Fix a timestep  $\Delta t$  for the tracking controller so that, e.g.,  $\mathbf{x}_t$  denotes  $\mathbf{x}(t \cdot \Delta t)$ , and fix a nominal trajectory  $(\mathbf{x}^{\text{nom}}(t), \mathbf{u}^{\text{nom}}(t), \mathbf{y}^{\text{nom}}(t))$ ,  $t \in [0, \tau]$  satisfying the dynamics (1) without the noise terms  $\mathbf{v}$  and  $\mathbf{w}$ . With deviation variables defined as  $\delta \mathbf{x}_t := \mathbf{x}_t - \mathbf{x}_t^{\text{nom}}$ ,  $\delta \mathbf{u}_t := \mathbf{u}_t - \mathbf{u}_t^{\text{nom}}$ , and  $\delta \mathbf{y}_t := \mathbf{y}_t - \mathbf{y}_t^{\text{nom}}$ , for  $t = 0, \dots, T$ , the tracking controller satisfies the discrete time system

$$\begin{aligned} \delta \mathbf{x}_{t+1} &= A \delta \mathbf{x}_t + B \delta \mathbf{u}_t + \mathbf{v}_t, \quad \mathbf{v}_t \sim \mathcal{N}(\mathbf{0}, V), \quad \delta \mathbf{y}_t = C \delta \mathbf{x}_t + \mathbf{w}_t, \quad \mathbf{w}_t \sim \mathcal{N}(\mathbf{0}, W), \\ A &:= e^{A_c \Delta t}, \quad B := \left( \int_0^{\Delta t} e^{A_c s} ds \right) B_c, \quad C := C_c, \quad V := \int_0^{\Delta t} e^{A_c s} V_c e^{A_c^\top s} ds, \quad W := \frac{W_c}{\Delta t}. \end{aligned} \quad (2)$$

The discrete LQG controller  $\delta \mathbf{u}_t^{\text{LQG}} := L_t \widehat{\delta \mathbf{x}}_t$ , with  $L_t$  and  $\widehat{\delta \mathbf{x}}_t$  denoting the feedback gain matrix and Kalman state estimate respectively (see [22] for computation details), minimizes the tracking cost  $J := \mathbb{E} \left[ \delta \mathbf{x}_T^\top F \delta \mathbf{x}_T + \sum_{t=0}^{T-1} \delta \mathbf{x}_t^\top Q \delta \mathbf{x}_t + \delta \mathbf{u}_t^\top R \delta \mathbf{u}_t \right]$ .

Then the total control applied in continuous time is  $\mathbf{u}(t) = \mathbf{u}^{\text{nom}}(t) + \delta \mathbf{u}_{\lfloor t/\Delta t \rfloor}^{\text{LQG}}$ .

The SKP problem is posed as a cost optimization over dynamically-feasible trajectories (also referred to as motion plans) subject to a safety tolerance constraint separate from the optimization objective. Let  $\mathcal{X}_{\text{obs}}$  be the obstacle space, so that  $\mathcal{X}_{\text{free}} = \mathbb{R}^d \setminus \mathcal{X}_{\text{obs}}$  is the free configuration space. Let  $\mathcal{X}_{\text{goal}} \subset \mathcal{X}_{\text{free}}$  and  $\mathbf{x}_0 = x_{\text{init}} \in \mathcal{X}_{\text{free}}$  be the goal region and initial state, respectively. Given a trajectory cost measure  $c$  and CP tolerance  $\alpha$ , we wish to solve the

#### Stochastic Kinodynamic Motion Planning (SKP):

$$\begin{aligned} \min_{\mathbf{u}^{\text{nom}}(\cdot)} \quad & c(\mathbf{x}^{\text{nom}}(\cdot)) \\ \text{s.t.} \quad & \mathbb{P}(\{x(t) \mid t \in [0, \tau]\} \cap \mathcal{X}_{\text{obs}} \neq \emptyset) \leq \alpha \\ & \mathbf{u}(t) = \mathbf{u}^{\text{nom}}(t) + \delta \mathbf{u}_{\lfloor t/\Delta t \rfloor}^{\text{LQG}} \\ & \text{Equation (1).} \end{aligned} \quad (3)$$

The numerical experiments in this work take  $c$  as the mixed time/quadratic control effort penalty studied in [23, 24]. We make an implicit assumption in optimizing over the cost of the reference trajectory  $c(\mathbf{x}^{\text{nom}}(\cdot))$  that the tracking control costs are minor in comparison to the nominal control cost; as noted in Section 1 this assumption also underlies the use of a tracking control strategy rather than computing a full policy over state beliefs.

### 3 Collision Probability Approximation

This section discusses a key challenge in computing solutions for the SKP problem, that of efficiently and accurately assessing collision probability. As discussed in [2], Monte Carlo methods exist as an *exact* means for calculating the CP when tracking a trajectory segment. These methods are suitable for validating the most promising candidate trajectories post-exploration, but the high branching factor of multiobjective search necessitates less computationally intensive approximation schemes when checking a great

number of candidate motions (most of which are discarded as Pareto dominated) in a tempo compatible with real-time operations. In Section 3.1 we briefly review existing strategies for approximating CP. In Section 3.2 we present the novel Half-Space Monte Carlo (HSMC) method aimed at efficiently and accurately approximating CP, particularly on GPUs, and analyze this method over a range of numerical experiments.

### 3.1 Additive, Multiplicative, and MC-based CP Approximations

While the constraint in (3) is defined over continuous trajectory realizations, there are a number of waypoint-based schemes which derive an approximation of policy CP as a function of the instantaneous pointwise collision probabilities at the intermediate waypoints  $\{\mathbf{x}_t\}$ . *Additive* approximations [7, 25, 26, 27] employ a conservative union bound

$$\text{CP} \approx \mathbb{P} \left( \bigvee_{t=0}^T \{\mathbf{x}_t \in \mathcal{X}_{\text{obs}}\} \right) \leq \sum_{t=0}^T \mathbb{P} (\{\mathbf{x}_t \in \mathcal{X}_{\text{obs}}\}), \quad (4)$$

while *multiplicative* approximations [8, 28, 29, 30] assume independence between pointwise collision events:

$$1 - \text{CP} \approx \mathbb{P} \left( \bigwedge_{t=0}^T \{\mathbf{x}_t \notin \mathcal{X}_{\text{obs}}\} \right) \approx \prod_{t=0}^T \mathbb{P} (\{\mathbf{x}_t \notin \mathcal{X}_{\text{obs}}\}). \quad (5)$$

This independence assumption may be relaxed by fitting Gaussians successively to the waypoint distributions conditioned on no prior collisions (see, e.g., [9, 31] for details), in order to approximate the terms of the product expansion

$$1 - \text{CP} \approx \mathbb{P} \left( \bigwedge_{t=0}^T \{\mathbf{x}_t \notin \mathcal{X}_{\text{obs}}\} \right) = \prod_{t=0}^T \mathbb{P} (\{\mathbf{x}_t \notin \mathcal{X}_{\text{obs}}\} \mid \bigwedge_{s=0}^{t-1} \{\mathbf{x}_s \notin \mathcal{X}_{\text{obs}}\}), \quad (6)$$

which we refer to in this text as the *conditional multiplicative* approximation. A common additional approximation made with these waypoint-based approaches is to assume a simplified collision model, for example by approximating the free space around a waypoint as an ellipsoid [7] or by a locally convex region defined by half-space constraints [31]. We note that even though these collision models, as well as the additive approximation (4), may be deemed conservative, none of these methods are guaranteed to over- or under-approximate the actual CP as they do not allow for collisions in the intervals between waypoints [2].

Monte Carlo methods can exactly address the dependencies between waypoint CPs, as well as accomodate continuous collision checking, at the expense of computational effort and statistical variance in the estimate. In [2], variance-reduced MC methods are developed for estimating CP along the span of a full trajectory tracking execution. Feedback-based Information RoadMap (FIRM) methods [6, 32] break dependence between collision probabilities at certain points in the configuration space using feedback controllers. This construct divides the CP computation into smaller pieces corresponding to local connections, which allows for accurate expensive Monte Carlo-based CP computation to be done offline, given the environment map.

### 3.2 Half-Space Monte Carlo

In this subsection we detail the massively parallel HSMC method and show that it attains good empirical accuracy. This CP approximation is inspired by particle-based MC methods in their ability to represent arbitrary state distributions and how they evolve in  $\mathcal{X}_{\text{free}}$ , as well as the efficient collision models of waypoint-based methods. Briefly, HSMC is a Monte Carlo method where, within local convex regions around a reference waypoint  $\mathbf{x}_t^{\text{nom}}$ , sampled trajectories (particles) are checked at each time step by removing those that might be “expected” to be in collision through subsequent motion towards  $\mathbf{x}_{t+1}^{\text{nom}}$ . Instead of computing a full collision check, we only compare the particle’s position in the workspace against the half-space boundaries of the local convex region, taking into account the reference waypoint state’s velocity. The local convexification process employed by HSMC differs from that presented in [31] and used in [2], in that obstacle half-spaces are computed on the basis of Euclidean distance in the workspace, as opposed to Mahalanobis distance. In those works Mahalanobis distance is used as a proxy for the shape of the uncertainty distribution centered at  $\mathbf{x}_t^{\text{nom}}$ ; HSMC instead maintains a discretized Monte Carlo representation of this uncertainty distribution so that position and velocity are sufficient to judge approximate collision in the Euclidean workspace. We remark that this approach allows for the parallel computation of all locally convex regions at the start of planning, before the uncertainty distributions, or even the reference trajectory, are fixed (as is the case in multiobjective exploration).

Because we are restricting our attention to the workspace, recall that  $\mathbf{y}_t = C\mathbf{x}_t$  is projection of the state into the workspace. The construction of the local convex region around  $\mathbf{y}_t^{\text{nom}}$  is performed using a sequential process, following the work of [31]. At step  $i$ , we define  $\mathbf{d}_{t,i}$  as the vector from  $\mathbf{y}_t^{\text{nom}}$  to the closest obstacle point and prune away all obstacle geometry  $\mathbf{z}$  that lies in the half-space  $\mathbf{d}_{t,i}^\top (\mathbf{z} - \mathbf{y}_t^{\text{nom}}) > \mathbf{d}_{t,i}^\top \mathbf{d}_{t,i}$ . This procedure continues until all obstacle geometry has been removed. The process defines the local convex region, however the final approximate collision check should represent the notion that a particle is in collision with an obstacle only if it is both close and its motion is towards the obstacle. We thus alter these half-spaces, as illustrated in Fig. 1, by projecting them to be perpendicular to the direction of travel via

$$\mathbf{a}_{t,i} = \mathbf{d}_{t,i} - \left( \frac{\mathbf{d}_{t,i} \cdot \dot{\mathbf{y}}_t}{\dot{\mathbf{y}}_t \cdot \dot{\mathbf{y}}_t} \right) \dot{\mathbf{y}}_t. \quad (7)$$

The resulting collision constraint for an MC particle is then defined by  $\mathbf{a}_{t,i}^\top \delta \mathbf{y}_t > \mathbf{b}_{t,i}$ , where  $\mathbf{b}_{t,i} = \mathbf{a}_{t,i} \cdot \mathbf{a}_{t,i}$ . That is, to approximate the CP of a given motion plan we generate a set of  $N$  particle trajectories and compare their deviations  $\delta \mathbf{y}_t$  from the nominal trajectory at each time step to the local collision half-spaces. Every half-space check ( $\mathbf{a}_{t,i}, \mathbf{b}_{t,i}$ ) along a particle trajectory is independent of every other, requiring only a final OR reduction to determine the validity of a particle, thus this process is amenable to parallelization. The final CP approximation is obtained by counting the number of invalid particle trajectories and dividing by  $N$ .

The results in Fig. 2 show that over several planning problems, targeting collision probabilities ranging from 1% to 15%, HSMC outperforms conditional multiplicative in terms of CP approximation accuracy. While the HSMC CP approximation improves as the number of waypoints increases, conditional multiplicative’s conservative nature causes the CP approximation to degrade, in agreement with the results in [2].

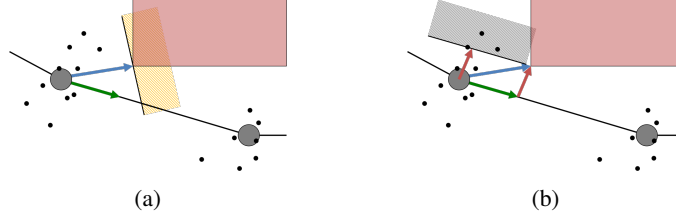


Fig. 1: The vector  $\mathbf{d}$  (blue) is the vector of minimum distance connecting the waypoint to the obstacle set and  $\dot{\mathbf{y}}$  (green) is the workspace velocity. (1a) Illustration of half-space formation by distance only. (1b) Illustration of the alteration of the half-space to account for motion; the vector  $\mathbf{a}$  (red) is computed as  $\mathbf{a} = \mathbf{d} - \left(\frac{\mathbf{d} \cdot \dot{\mathbf{y}}}{\dot{\mathbf{y}} \cdot \dot{\mathbf{y}}}\right) \dot{\mathbf{y}}$ .

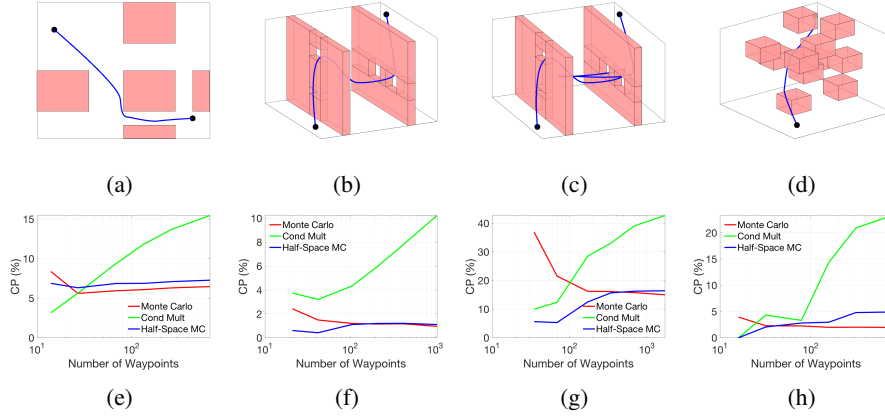


Fig. 2: Comparison of the true CP (Monte Carlo, red), conditional multiplicative CP approximation (green), and HSMC CP approximation (blue) versus number of waypoints (i.e. as the timestep  $\Delta t$  decreases) over several problem instances. Each HSMC approximation and MC CP was computed with 10,000 samples. Note that the conditional multiplicative approximation tends to become increasingly conservative as the number of waypoints increase, whereas HSMC generally remains near the true CP.

#### 4 Parallel Uncertainty-aware Multiobjective Planning

The Parallel Uncertainty-aware Multiobjective Planning (PUMP) algorithm explores the configuration space via a multiobjective search, building a Pareto optimal set of motion plans from the initial state to goal region, where Pareto dominance is determined by cost and approximated CP. This Pareto optimal set comprises not only several motion plans, but different solution homotopies, which are searched to find the minimum cost motion plan certified to satisfy a CP constraint. The algorithm is briefly outlined in Alg. 1 and formally stated in Algs. 2-5.

To aid in formal description, we now present some notation and algorithmic primitives. In line with the sampling-based motion planning literature, we construct motion plans as a sequence of sampled nodes (samples) in  $\mathbb{R}^d$ . Since we are interested



**Algorithm 1** Parallel Uncertainty-aware Multiobjective Planning: Outline

- 
- 1 Massively parallel sampling-based graph building
  - 2 Multiobjective search to find  $P_{\mathcal{X}_{\text{goal}}} :=$  Pareto optimal plans in terms of (cost, approx. CP)
  - 3 Bisection search  $P_{\mathcal{X}_{\text{goal}}}$  to find the best motion plan,  $p^*$ , with a verified CP below constraint  
     If feasible plan found, locally optimize (smooth) subject to CP constraint satisfaction  
     and return  $p^*$ , otherwise report failure
- 

in tracking collision probability, which is history dependent, we store plans as structs with attributes (head, path, cost,  $\hat{\text{cp}}$ ). The fields represent the terminal trajectory node from which we may extend other plans, the list of previous nodes, the cost, and the approximate CP, respectively. Let  $\text{SampleFree}(n)$  be a function that returns a set of  $n \in \mathbb{N}$  points sampled from  $\mathcal{X}_{\text{free}}$ . In the following definitions let  $u, v \in \mathcal{X}_{\text{free}}$  be samples, and let  $V \subset \mathcal{X}_{\text{free}}$  be a set of samples. Define  $\text{Cost}(u, v)$  as a function that returns the cost of the optimal trajectory from  $u$  to  $v$ . Let  $\text{Near}(V, u, r)$  be a function that returns the set of samples  $\{v \in V : \text{Cost}(u, v) < r\}$ . Let  $\text{Collision}(u, v)$  denote whether the optimal trajectory from  $u$  to  $v$  intersects  $\mathcal{X}_{\text{obs}}$ . Given a set of motion plans  $P$  and  $P_{\text{open}} \subset P$ ,  $\text{RemoveDominated}(P, P_{\text{open}})$  denotes a function that removes any  $p \in P_{\text{open}}$  from  $P_{\text{open}}$  and  $P$  if the tuple  $(p.\text{cost}, p.\hat{\text{cp}})$  is dominated by any motion plan in  $\{p_{\text{dom}} \in P : p_{\text{dom}}.\text{head} = p.\text{head}\}$ ; we say that  $p_{\text{dom}}$  dominates  $p$  if  $(p.\text{cost} < p_{\text{dom}}.\text{cost}) \wedge (p.\hat{\text{cp}} < p_{\text{dom}}.\hat{\text{cp}})$ . Let  $\text{CP}(v, p)$  denote a function that returns an approximate CP for the motion plan  $p$  concatenated with the optimal connection  $p.\text{head}$  to  $x$ . We define  $\text{MC}(p)$  as a function that returns an unbiased CP estimate of motion plan  $p$  through Monte Carlo sampling [2]. Since PUMP conducts its exploration phase within the context of a discrete graph representation of  $\mathcal{X}_{\text{free}}$ , the best costs and  $\hat{\text{cp}}$  that phase can return are limited by the resolution of the graph. In order to address variance in sample placement, we include a post-processing “smoothing” step which locally optimizes the final plan subject to constraint ( $\text{CP} \leq \alpha$ ) recertification. We denote this process by  $\text{Smooth}(p, \alpha)$ ; in this work we use the strategy introduced in [33], which performs a bisection search to create a new smoothed motion plan as a combination of the original motion plan and the optimal unconstrained trajectory from  $x_{\text{init}}$  to  $p.\text{head}$ .

We are now ready to fully detail the PUMP algorithm (Algs. 2-5). The main body is provided in Alg. 2; for clarity we assume the algorithm inputs and tuning parameters are available globally to the subroutines Algs. 3-5. PUMP can be divided into three phases, the first is a graph building phase (Alg. 3), similar to probabilistic roadmap methods [13], that constructs a representation of available motions within the free configuration space. This phase begins by adding  $x_{\text{init}}$  and a set of  $n$  samples from  $\mathcal{X}_{\text{free}}$  (including at least one from  $\mathcal{X}_{\text{goal}}$ ) to the set of samples  $V$ . Each sample’s nearest neighbors are then computed and each neighbor edge is collision checked, storing the collision-free neighbors of  $v$  in  $N(v)$ . Depending on the CP approximation strategy used for the exploration phase, this graph building stage can also calculate obstacle half-spaces for each edge. Following the discussion in [13], this first phase is embarrassingly parallel.

The second phase of the algorithm, Alg. 4, explores the configuration space to find the Pareto optimal set of motion plans, where Pareto dominance is determined in terms of cost and  $\hat{\text{cp}}$ . This phase takes an upper and lower bound,  $\alpha_{\text{max}}$  and  $\alpha_{\text{min}}$ , expressed in terms of  $\hat{\text{cp}}$ . These bounds are chosen as a multiplicative factor  $\eta$  around the target CP to accomodate any under- or over-CP approximation;  $\eta$  may be tuned according to the

**Algorithm 2** Parallel Uncertainty-aware Multiobjective Planning

**Inputs:** planning problem  $(\mathcal{X}_{\text{free}}, x_{\text{init}}, \mathcal{X}_{\text{goal}})$ , number of nodes  $n \in \mathbb{N}$ ,  
connection radius  $r_n \in \mathbb{R}_{\geq 0}$ , CP constraint  $\alpha \in (0, 1)$

**Parameters:** CP approximation factor  $\eta > 1$ , group cost threshold  $\lambda \in (0, 1]$

---

```

1  $(V, N) = \text{BuildGraph}()$  // parallel graph building, Alg. 3
2  $\alpha_{\min} = \frac{1}{\eta}\alpha; \alpha_{\max} = \eta\alpha$ 
3  $P_{\mathcal{X}_{\text{goal}}} \leftarrow \text{Explore}(\alpha_{\min}, \alpha_{\max}, V, N)$  // find Pareto optimal plans, Alg. 4
4  $p^* \leftarrow \text{PlanSelection}(\alpha, P_{\mathcal{X}_{\text{goal}}})$  // select best plan with true CP below  $\alpha$ , Alg. 5
5 return  $p^*$ 

```

---

**Algorithm 3** *BuildGraph*


---

```

1  $V \leftarrow \{x_{\text{init}}\} \cup \text{SampleFree}(n)$ 
2 for all  $v \in V$  do // massively parallel graph building phase
3    $N(v) \leftarrow \text{Near}(V \setminus \{v\}, v, r_n)$ 
4   for all  $u \in N(v)$  do
5     if  $\text{Collision}(v, u)$  then
6        $N(v) \leftarrow N(v) \setminus \{u\}$ 
7     end if
8   end for
9 end for
10 return  $(V, N)$ 

```

---

accuracy of  $\widehat{\text{CP}}$ . The exploration of the configuration space proceeds in a parallel fashion by expanding the group,  $\mathcal{G}$ , of all open (unexpanded) motion plans,  $P_{\text{open}}$ , below an increasing cost threshold, to their nearest neighbors. During this process we discard any motion plans that are dominated or have  $\widehat{\text{cp}} > \alpha_{\max}$ . The cost threshold is increased by  $\lambda r_n$  at each exploration loop; the size of  $\mathcal{G}$  is thus determined by the factor  $\lambda \in (0, 1]$ . The exploration terminates once a plan reaches  $\mathcal{X}_{\text{goal}}$  with  $\widehat{\text{cp}} < \alpha_{\min}$  or once  $P_{\text{open}} = \emptyset$ , at which point all plans connecting  $x_{\text{init}}$  to  $\mathcal{X}_{\text{goal}}$  are stored in  $P_{\mathcal{X}_{\text{goal}}}$ . The  $\alpha_{\min}$  early termination criterion introduces a tradeoff for  $\lambda$ : choosing a high  $\lambda$  increases algorithm speed through greater parallelism, but has the side effect of allowing  $P_{\text{open}}$  to spread out in cost, potentially terminating before a high quality partial plan has reached  $\mathcal{X}_{\text{goal}}$ . Finally, we note that the discretization of the expansion groups has an added benefit of not requiring a heap to store a cost ordering on  $P_{\text{open}}$ , but rather a calendar queue [34] should be implemented, allowing  $\mathcal{O}(1)$  insertion and removal.

Computational tractability of PUMP relies on the use of the `RemoveDominated` function, and thus it is important to discuss its associated assumptions. Pruning the search requires judging the potential of multiple candidate plans that arrive at the same node. We use each plan's  $\widehat{\text{cp}}$  for this purpose, but this disregards any impact of the shape of the plan's full probability distribution, conditioned on prior obstacle avoidance, at that node. We note that even an exact CP estimate would be insufficient for this purpose. The only remedy is an utterly exhaustive search; instead our goal during the exploration

**Algorithm 4** *Explore*( $\alpha_{\min}, \alpha_{\max}, V, N$ )

---

```

1  $P_{\text{open}} \leftarrow \{(x_{\text{init}}, \emptyset, 0, 0)\}$  // motion plans ready to be expanded
2  $P(x_{\text{init}}) \leftarrow P_{\text{open}}$  // motion plans with head at  $x_{\text{init}}$ 
3  $\mathcal{G} \leftarrow P_{\text{open}}$  // motion plans considered for expansion
4  $i = 0$ 
5 while  $P_{\text{open}} \neq \emptyset \wedge \{g \in \mathcal{G} : (g.\text{head} \in \mathcal{X}_{\text{goal}}) \wedge (g.\text{cp} < \alpha_{\min})\} = \emptyset$  do
6   for all  $p \in \mathcal{G}$  do
7     for all  $x \in N(p.\text{head})$  do
8        $q \leftarrow (x, p.\text{path} + \{p.\text{head}\}, p.\text{cost} + \text{Cost}(p.\text{head}, x), \widehat{\text{CP}}(x, p))$ 
9       if  $q.\text{cp} < \alpha_{\max}$  then // CP cutoff
10         $P(x) \leftarrow P(x) \cup \{q\}$ 
11         $P_{\text{open}} \leftarrow P_{\text{open}} \cup \{q\}$ 
12      end if
13    end for
14  end for
15   $(P, P_{\text{open}}) \leftarrow \text{RemoveDominated}(P, P_{\text{open}})$ 
16   $P_{\text{open}} \leftarrow P_{\text{open}} \setminus \mathcal{G}$ 
17   $i \leftarrow i + 1$ 
18   $\mathcal{G} \leftarrow \{p \in P_{\text{open}} : p.\text{cost} \leq i\lambda r_n\}$ 
19 end while
20 return  $P_{\mathcal{X}_{\text{goal}}} \leftarrow \{p \in P(v) : v \in \mathcal{X}_{\text{goal}}\}$ 

```

---

**Algorithm 5** *PlanSelection*( $\alpha, P_{\mathcal{X}_{\text{goal}}}$ )

---

```

1  $P \leftarrow \text{Sort}(P_{\mathcal{X}_{\text{goal}}})$  // Sort  $P_{\mathcal{X}_{\text{goal}}}$  in ascending  $\widehat{\text{CP}}$  order
2  $l = 1, u = |P_{\mathcal{X}_{\text{goal}}|}, m = \lceil (l + u)/2 \rceil$ 
3 while  $l \neq u$  do
4   if  $\text{MC}(P_m) > \alpha$  then
5      $u = m - 1$ 
6   else
7      $l = m$ 
8   end if
9    $m = \lceil (l + u)/2 \rceil$ 
10 end while
11 if  $\text{MC}(P_m) > \alpha$  then
12   return Failure // No feasible plans in  $P_{\mathcal{X}_{\text{goal}}}$ 
13 end if
14 return  $\text{Smooth}(P_m, \alpha)$ 

```

---

phase is to produce a set of high-quality motion plans. We find that in practice, using  $\widehat{\text{CP}}$ 's, this set encompasses all important trajectory homotopy classes.<sup>1</sup>

The third and final phase of the algorithm, Alg. 5, performs a bisection search over  $P_{\mathcal{X}_{\text{goal}}}$  to identify the lowest cost solution  $p^*$  with a CP certifiably below  $\alpha$ , as veri-

---

<sup>1</sup> We note here an additional potential source of algorithm suboptimality — the fact that we search over a graph of only cost-optimal  $u$ - $v$  connections. In some cases, e.g., high initial uncertainty compared to the steady-state, it may be best to consider other strategies for local connection, e.g., waiting if possible.

fied through MC simulation with full collision checking [2]. If no suitable motion plan is found, the algorithm reports failure. Otherwise, we return  $\text{Smooth}(p^*, \alpha)$ , detailed above, which reduces cost until any margin in the CP constraint is exhausted.

## 5 Numerical Experiments

### 5.1 Experimental Setup

The experiments in this section were written in CUDA C and generated on an NVIDIA GeForce GTX 980 GPU on a Unix system with a 3.0 GHz CPU. Some implementation details have been omitted in the discussion below; source code for these results can be accessed at <https://github.com/StanfordASL/PUMP>.

The simulations in this section use 6D double integrator dynamics ( $\ddot{x} = u$ ) to model a quadrotor system in a 3D workspace. We implemented configuration space sampling with the deterministic, low-dispersion Halton sequence, as motivated by the analysis in [35]. By allocating GPU memory offline and caching nearest-neighbors and edge controls (both independent of the particular problem instance  $\mathcal{X}_{\text{obs}}$ ), the total run time was significantly reduced. The HSMC CP approximation method detailed in Section 3.2 was used in *Explore* (Alg. 4), with the CP approximation factor  $\eta$  and number of HSMC particles  $N$  left as tuning parameters (for example at a 1% target CP we use  $\eta = 2$ , and for all the simulations below we set  $N = 128$ ). Note that the number of HSMC particles tracked may be quite low as it is solely used to guide the exploration phase towards promising motion plans rather than certify solutions. Lastly, we set a group factor of  $\lambda = 0.5$ , though this too can also be considered a tuning parameter.

### 5.2 Comparison to Monte Carlo Motion Planning

We begin with a discussion of Monte Carlo Motion Planning (MCMP) [2], a recent approach to solving the SKP problem, and show that PUMP identifies significantly lower cost solutions in a pair of illustrative examples. MCMP addresses the SKP problem by performing a bisection search over a safety-buffer heuristic correlated with CP, at each step solving a deterministic planning problem with inflated obstacles (higher inflation factor correlates with lower trajectory CP). While [2] argues that the algorithm works well in many cases, the assumption that safety-buffer distance is a good analogue for CP breaks down in some planning problems. We show two such examples in Figs. 3a and 3d and show that PUMP’s  $\widehat{\text{CP}}$ -guided multiobjective search outperforms MCMP.

Figure 3a displays a planning problem in which the solution trajectory CP increases as inflation factor increases (Fig. 3b). This is a consequence of a narrow, but short gap allowing safer trajectories than a wide, but long passage. When iterating on inflation factor, the MCMP algorithm is unable to locate the solution homotopy class through the narrow gap, as the inflated obstacles block it. Figure 3c shows the cost of solutions for various target CPs as compared to PUMP, which identifies the narrow gap solution for all CPs. For CPs below 3%, the narrow gap is never identified and instead a more circuitous motion plan is obtained. MCMP’s performance is particularly troublesome with a 0.1% target CP, in which case MCMP is unable to find any solution as the long passage homotopy class is infeasible, never realizing the narrow gap homotopy class.

The second planning problem, shown in Fig. 3d, admits two solution homotopies: a narrow passage and a large open region. Figure 3e shows that as the inflation factor is varied, there is a large discontinuity in CP when the narrow gap becomes blocked. Thus, if the targeted CP is within this gap, the algorithm will converge to exactly the inflation factor that minimally blocks the gap, alternating between motion plans through the narrow passage with high CPs and overly conservative motion plans through the open region, not identifying the desired aggressive motion plan through the open region. Figure 3f shows that PUMP is able to find this solution through the open region (unless the gap homotopy is valid for a target CP) while MCMP is overly conservative, especially at low target CPs. A homotopy blocking heuristic is suggested in [2] for remedying this issue, but this is difficult to execute for planning in general 3D workspaces.

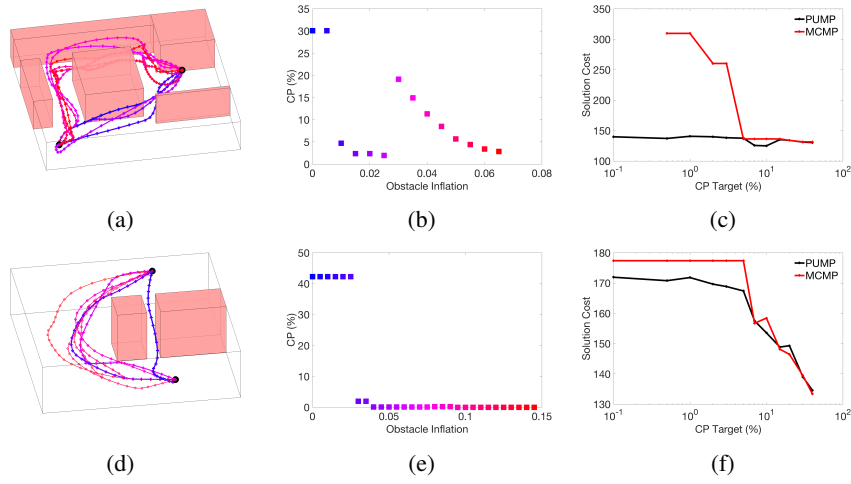


Fig. 3: MCMP and PUMP comparisons. (3a) and (3d) plot MCMP candidate plans at a range of safety buffers. (3a-3c) In this case CP actually increases as inflation factor increases causes MCMP to not find the optimal solution homotopy. PUMP is able to find the best homotopy at all CPs. Note that MCMP fails to find a solution at a CP of 0.1% due to not identifying the narrow, short gap before the wide, long passageway is closed. (3d-3f) A gap in the CP causes MCMP to not be aggressive enough through the open region at low CPs, while PUMP successfully identifies this solution.

### 5.3 Real-Time Performance and Homotopy Identification

Through the two planning problems in Fig. 4, we demonstrate PUMP’s ability to identify multiple solution homotopy classes and select low-cost trajectories subject to a certified CP constraint, all in a tempo compatible with real-time application ( $\sim 100$  ms). The collision probability constraints considered herein are single digit percentages and below, as has been studied for realistic stochastic planning problems in the literature [9]. Table 1 details the resulting computation times, solution CPs, and number of partial plans considered, over a range of target CPs and graph sample counts. In Table 1 we also present results for a simple repeated RRT method for generating candidate plans.

For this comparison, we compute 1000 kinodynamic RRT solution trajectories (as performed in [8]) and select the trajectory with lowest cost subject to MC certification of chance constraint satisfaction. In all cases PUMP execution times are on the order of 100 ms, while considering order one hundred thousand partial trajectories in the multi-objective search. Note that these solution times are two orders of magnitude faster than those reported for MCMP [2], owing to the parallel algorithm design and implementation on GPU hardware. On average, the graph construction accounted for 17% of the total run time, the exploration for 79% (55% overall for running HSMC), and only 4% for the final trajectory selection, smoothing, and certification phase.

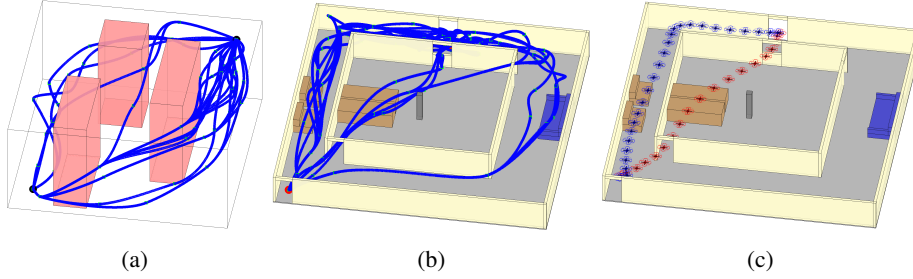


Fig. 4: (4a-4b) Illustration of candidate motion plans identified by PUMP’s exploration phase, representing multiple homotopy classes. (4c) Chosen trajectories for a 2% (blue) and 5% (red) target CP; the 2% CP motion plan takes a less aggressive route.

Table 1: PUMP vs. repeated RRT (1000 trials) double integrator experimental results.

Target CP (%)	Figure 4a									Figure 4b-4c					
	0.1			1			5			2			5		
Sample Count	4k	6k	8k	4k	6k	8k	4k	6k	8k	2k	3k	4k	2k	3k	4k
Solution CP (%)	0.10	0.10	0.10	1.00	1.00	1.00	5.00	5.00	5.00	1.95	1.95	1.90	4.98	4.93	4.93
Cost	2.11	2.11	2.11	2.02	2.02	2.08	1.97	1.97	1.88	3.41	2.41	1.85	1.48	1.31	1.31
Time (ms)	48	122	216	82	183	323	79	223	261	97	253	282	99	224	384
Partial Plans	81k	288k	554k	130k	367k	700k	157k	570k	600k	120k	284k	456k	152k	331k	641k
rRRT CP (%)	no satisfactory			0.98			3.52			no satisfactory			no satisfactory		
rRRT Cost	plan found			2.89			2.22			plan found			plan found		

Figure 4a shows the first of the planning problems, in which PUMP’s multiobjective search phase has identified all important solution homotopies. The little variation in cost with graph resolution (i.e., sample count) demonstrates that PUMP generally identifies not only the correct homotopy, but as aggressive a solution as possible within it. Repeated RRT did not encounter a candidate plan with CP below 0.1%, and achieved significantly worse cost than PUMP’s principled search for target CPs 1% and 5%.

The second planning problem is structured as an indoor flight scenario, once again with multiple solution homotopy classes. Figure 4b shows the workspace setup and the Pareto optimal set of trajectories, representing several homotopies, identified by PUMP’s multiobjective search. Targeting CPs of 2% and 5%, the results shown in Table 1 demonstrate that even in this more complex workspace, PUMP still finds solutions tightly bound on the CP constraint with computation times on the order of 100

ms. Unlike the previous example, however, as the search in Fig. 4b is performed at lower sample counts, a trend of increasing solution quality as graph resolution increases is observed, possibly reflecting the more complex obstacle environment. Figure 4c illustrates the cost tradeoff for a 2% (blue) and 5% (red) target CP, in which the 2% motion plan must take a more conservative and costly route (routes visualized through time at <https://www.youtube.com/watch?v=ac4A4-ctqrM>). Repeated RRT did not identify any candidate plans below 5% CP in this tight hallway environment; the lowest trajectory CP found was 9.57% with a cost of 1.86.

## 6 Conclusions

In this paper we have introduced the Parallel Uncertainty-aware Multiobjective Planning algorithm for chance-constrained motion planning. PUMP represents, to the best of our knowledge, an algorithmic first in that it directly considers both cost and collision probability at equal priority when planning through the free configuration space. Although multiobjective search is computationally intensive, we have demonstrated that a combination of algorithm design and parallel hardware implementation allows for this principled approach to achieve run times compatible with a  $\sim 10$  Hz planning loop. Included in the PUMP run time is a Monte Carlo-based certification step to guarantee the collision probability constraint is met, without sacrificing cost metric performance due to conservatism beyond the safety design constraints. The Half-Space Monte Carlo method used in our PUMP experiments may also be of general interest as an empirically accurate and fast way to approximate motion plan CP.

This work leaves many avenues for further investigation. First, we plan to implement this algorithm for more varied dynamical systems and uncertainty models to verify its generality. Second, we plan to extend this algorithm to environmental uncertainty, particularly in dynamically evolving environments. Third, we plan to extend the presented multiobjective methodology to other constraints, such as arrival time windows and resource constraints. Finally, we are in the process of implementing and verifying this algorithm and problem setup onboard a GPU-equipped quadrotor.

**Acknowledgments** Brian Ichter was supported by the Department of Defense (DoD) through the National Defense Science & Engineering Graduate Fellowship (NDSEG) Program. This work was supported by a Qualcomm Innovation Fellowship and by NASA under the Space Technology Research Grants Program, Grant NNX12AQ43G.

## References

- [1] S. Lavalle, *Planning Algorithms*. Cambridge University Press, 2006.
- [2] L. Janson, E. Schmerling, and M. Pavone, “Monte Carlo Motion Planning for Robot Trajectory Optimization Under Uncertainty,” in *International Symposium on Robotics Research*, 2015.
- [3] L. P. Kaelbling, M. L. Littman, and A. Cassandra, “Planning and acting in partially observable stochastic domains,” *Artificial Intelligence*, 1998.
- [4] H. Kurniawati, D. Hsu, and W. S. Lee, “SARSOP: Efficient point-based POMDP planning by approximating optimally reachable belief spaces,” in *Robotics: Science and Systems*, 2008.
- [5] T. Lee and Y. J. Kim, “Massively parallel motion planning algorithms under uncertainty using POMDP,” *International Journal of Robotics Research*, 2015.
- [6] A. Agha-Mohammadi, S. Chakravorty, and N. M. Amato, “FIRM: Sampling-based feedback motion planning under motion uncertainty and imperfect measurements,” *International Journal of Robotics Research*, 2014.

- [7] B. Luders, M. Kothari, and J. P. How, "Chance constrained RRT for probabilistic robustness to environmental uncertainty," in *AIAA Conf. on Guidance, Navigation and Control*, 2010.
- [8] J. V. D. Berg, P. Abbeel, and K. Goldberg, "LQG-MP: Optimized path planning for robots with motion uncertainty and imperfect state information," *International Journal of Robotics Research*, 2011.
- [9] W. Sun, S. Patil, and R. Alterovitz, "High-Frequency Replanning Under Uncertainty Using Parallel Sampling-Based Motion Planning," *IEEE Transactions on Robotics*, 2015.
- [10] L. Blackmore, M. Ono, A. Bektassov, and B. C. Williams, "A probabilistic particle-control approximation of chance-constrained stochastic predictive control," *IEEE Transactions on Robotics*, 2010.
- [11] N. Alechina and B. Logan, "State space search with prioritised soft constraints," *Applied Intelligence*, 2001.
- [12] P. Sanders and L. Mandow, "Parallel label-setting multi-objective shortest path search," in *Parallel & Distributed Processing*, 2013.
- [13] N. M. Amato and L. K. Dale, "Probabilistic Roadmap Methods Are Embarrassingly Parallel," in *Proc. IEEE Conf. on Robotics and Automation*, 1999.
- [14] J. Pan, C. Lauterbach, and D. Manocha, "g-Planner: Real-time Motion Planning and Global Navigation using GPUs," in *AAAI Conf. on Artificial Intelligence*, 2010.
- [15] —, "Efficient Nearest-Neighbor Computation for GPU-based Motion Planning," in *IEEE/RSJ Int. Conf. on Intelligent Robots & Systems*, 2010.
- [16] J. Bialkowski, S. Karaman, and E. Frazzoli, "Massively Parallelizing the RRT and the RRT\*," in *IEEE/RSJ Int. Conf. on Intelligent Robots & Systems*, 2011.
- [17] D. Devaurs, T. Siméon, and J. Cortés, "Parallelizing RRT on Large-scale Distributed-Memory Architectures," *IEEE Transactions on Robotics*, 2013.
- [18] C. Park, J. Pan, and D. Manocha, "Poisson-RRT," in *Proc. IEEE Conf. on Robotics and Automation*, 2014.
- [19] O. Cetin and G. Yilmaz, "Real-time Autonomous UAV Formation Flight with Collision and Obstacle Avoidance in Unknown Environment," *Journal of Intelligent & Robotic Systems*, 2016.
- [20] C. Park, J. Pan, and D. Manocha, "Real-time Optimization-based Planning in Dynamic Environments Using GPUs," in *Proc. IEEE Conf. on Robotics and Automation*, 2013.
- [21] T. Lee, M. Leoky, and N. H. McClamroch, "Geometric tracking control of a quadrotor UAV on SE(3)," in *Proc. IEEE Conf. on Decision and Control*, 2010.
- [22] A. J. Shaiju and I. R. Petersen, "Formulas for Discrete Time LQR, LQG, LEQG and Minimax LQG Optimal Control Problems," in *IFAC World Congress*, 2008.
- [23] D. J. Webb and J. van den Berg, "Kinodynamic RRT\*: Optimal Motion Planning for Systems with Linear Differential Constraints," in *Proc. IEEE Conf. on Robotics and Automation*, 2013.
- [24] E. Schmerling, L. Janson, and M. Pavone, "Optimal Sampling-Based Motion Planning under Differential Constraints: the Drift Case with Linear Affine Dynamics," in *Proc. IEEE Conf. on Decision and Control*, 2015.
- [25] G. S. Aoude, B. D. Luders, J. M. Joseph, N. Roy, and J. P. How, "Probabilistically safe motion planning to avoid dynamic obstacles with uncertain motion patterns," *Autonomous Robots*, 2013.
- [26] M. Kothari and I. Postlethwaite, "A probabilistically robust path planning algorithm for UAVs using rapidly-exploring random trees," *Journal of Intelligent & Robotic Systems*, 2013.
- [27] B. D. Luders, S. Karaman, and J. P. How, "Robust sampling-based motion planning with asymptotic optimality guarantees," in *AIAA Conf. on Guidance, Navigation and Control*, 2013.
- [28] N. Toit and J. Burdick, "Robotic motion planning in dynamic, cluttered, uncertain environments," in *Proc. IEEE Conf. on Robotics and Automation*, 2010.
- [29] W. Liu and M. H. Ang, "Incremental Sampling-Based Algorithm for Risk-Aware Planning Under Motion Uncertainty," in *Proc. IEEE Conf. on Robotics and Automation*, 2014.
- [30] A. Censi, D. Calisi, A. D. Luca, and G. Oriolo, "A bayesian framework for optimal motion planning with uncertainty," in *Proc. IEEE Conf. on Robotics and Automation*, 2008.
- [31] S. Patil, J. van den Berg, and R. Alterovitz, "Estimating probability of collision for safe motion planning under Gaussian motion and sensing uncertainty," in *Proc. IEEE Conf. on Robotics and Automation*, 2012.
- [32] A. Agha-mohammadi, S. Agarwal, S. Chakravorty, and N. M. Amato, "Simultaneous localization and planning for physical mobile robots via enabling dynamic replanning in belief space," *Computing Research Repository*, 2015.
- [33] J. A. Starek, E. Schmerling, G. D. Maher, B. W. Barbee, and M. Pavone, "Fast, Safe, and Propellant-Efficient Spacecraft Motion Planning under CWH Dynamics," *AIAA Journal of Guidance, Control, and Dynamics, Special Issue on Computational Guidance and Control*, 2016, in Press.
- [34] R. Brown, "Calendar queues: a fast  $O(1)$  priority queue implementation for the simulation event set problem," *Communications of the ACM*, 1988.
- [35] L. Janson, B. Ichter, and M. Pavone, "Deterministic Sampling-Based Motion Planning: Optimality, Complexity, and Performance," in *International Symposium on Robotics Research*, 2015.